Epitaxial growth mechanism of $L1_0$ FePt thin films on Pt/Cr bilayer with amorphous glass substrate

An-Cheng Sun and P. C. Kuo
Institute of Materials Science and Engineering, National Taiwan University, Taipei 106, Taiwan

Jen-Hwa Hsu[a] and H. L. Huang
Department of Physics, National Taiwan University, Taipei 106, Taiwan

Jui-Ming Sun
Department of Surgery, Songshan Armed Forces Hospital, Taipei 105, Taiwan

(Received 13 June 2005; accepted 24 August 2005; published online 14 October 2005)

Ordered $L1_0$ FePt films with magnetic perpendicular anisotropy were fabricated with a Pt/Cr bilayer. The squareness of the $L1_0$ FePt film with a Cr underlayer and a Pt buffer was close to one when a magnetic field was applied perpendicular to the film's plane, because a semicoherent epitaxial growth was initiated from the Cr (002) underlayer; continued through the Pt buffer layer, and extended into the $L1_0$ FePt (001) magnetic layer. Without the Pt buffer layer, the Cr atoms may diffuse directly into the FePt magnetic layer. Consequently, an epitaxial barrier of the Cr-rich FePtCr alloy formed between the Cr underlayer and the FePt magnetic layer, degrading the magnetic performance and epitaxial growth of the latter. © *2005 American Institute of Physics*.
[DOI: 10.1063/1.2073967]

The perpendicular magnetic anisotropic (PMA) FePt alloy thin film with a tetragonal $L1_0$ structure has attracted much interest in recent years,[1–5] because of its high uniaxial magnetocrystalline anisotropy (K_u), high coercivity (H_c), high saturation magnetization (M_s), good corrosive resistance, and large energy products $(BH)_{max}$.[6–8] The uniaxial magnetocrystalline anisotropic energy of the $L1_0$ FePt phase is close to 10^8 erg/cm^3, which is one order of magnitude greater than that of the Co-based alloy thin films.[6] The stable FePt grains can be as small as 2.8 nm, and thus overcome the thermal instability that causes superparamagnetism,[6] helping meet the criteria associated with the Stoner-Wohlfarth model.[9] Therefore, $L1_0$ FePt is a promising replacement for the Co-based alloy thin films used as ultrahigh magnetic recording density media in the near future. However, the tetragonal $L1_0$ FePt phase normally has a (111) plane and its easy axis is tilted 35° away from the film's plane. The preferred orientation must have a (001) plane that makes the easy axis [001] perpendicular to the film, to enable FePt to be used as a perpendicular recording media. Accordingly, a unique method of preparation that switches the preferred orientation of the ordered $L1_0$ FePt phase from (111) to (001) must be developed.

The lattice constant of MgO is 4.21 Å,[8] and the lattice mismatch[10] of the FePt(001)/MgO(100) planes is around 9.07%. Therefore, the MgO(100) substrate and MgO(100) thin film are widely employed to induce the ordered FePt(001) during growth. However, the cost of using the MgO(100) substrate is high and the fabrication temperature of MgO(100) thin film always exceeds 500 °C,[11,12] limiting the adoption of MgO in the magnetic recording industry. A perpendicular FePt(001) structure with a CrRu underlayer has been proposed.[1,13–15] The application of a CrRu underlayer is also limited by its huge material cost, although such underlayers have been investigated comprehensively.[13–15] Cr is an alternative because it has already been utilized as an underlayer in longitudinal recording. The lattice mismatch of Cr(002)/FePt(001) is 5.8%, which is below 6.3% of the $Cr_{91}Ru_9$(002)/FePt(001) planes.[15] A smaller lattice mismatch between the Cr(002) and FePt(001) planes helps the Cr(002) underlayer induce the ordering of the FePt(001) plane. However, no investigation has used a pure Cr layer as an underlayer for growing ordered FePt(001). In this work, ordered $L1_0$ FePt(001) grew epitaxially in the FePt/Pt/Cr trilayer, but not in the FePt/Cr bilayer. This article proposed the mechanism of formation of ordered $L1_0$ FePt with a (001) orientation and interfacial epitaxial characteristics.

All of the films were deposited on a preheated Corning glass substrate by conventional dc magnetron sputtering. Table I provide the film structures. The magnetic properties were measured using a vibrating-sample magnetometer (VSM) at room temperature. The crystalline phases and cross-sectional microstructures of the films were identified by x-ray diffraction (XRD) using Cu K_α radiation and 300 KeV high-resolution transmission electron microscopy (HR-TEM). The chemical composition of the magnetic FePt alloy layer, which was determined by energy dispersive x-ray dif-

TABLE I. Film structures of samples A–E.

Sample ID	Film structures
A	Cr(90 nm)/glass
B	FePt(20 nm)/glass
C	FePt(20 nm)/Cr(90 nm)/glass
D	FePt(20 nm)/Pt(2 nm)/glass
E	FePt(20 nm)/Pt(2 nm)/Cr(90 nm)/glass

[a]Author to whom correspondence should be addressed; FAX:886-2-33665892; electronic mail: jhhsu@phys.ntu.edu.tw

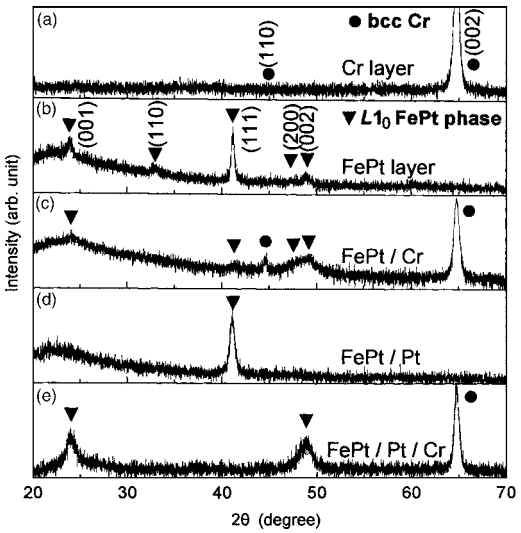

FIG. 1. XRD patterns of (a) sample A (single Cr layer), (b) sample B (single FePt layer), (c) sample C (FePt/Cr bilayer), (d) sample D (FePt/Pt bilayer), and (e) sample E (FePt/Pt/Cr trilayer).

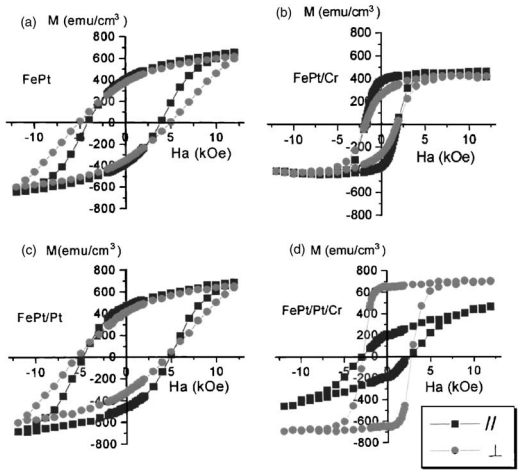

FIG. 2. Magnetic hysteresis loops of (a) sample B (single FePt layer), (b) sample C (FePt/Cr bilayer), (c) sample D (FePt/Pt bilayer), and (d) sample E (FePt/Pt/Cr trilayer).

fractometry (EDX), was found to be $Fe_{48}Pt_{52}$. The depth profiles of the composition were examined by Auger electron spectroscopy (AES).

Figure 1 presents the x-ray diffraction patterns of samples A–E. Figure 1(a) (sample A) has no Cr(110) peak, but includes a high-intensity Cr(002) peak, revealing that the orientation of the (002) plane Cr underlayer is favorable. In Fig. 1(b), the multiple peaks indicate a randomly oriented $L1_0$ FePt phase with a preferred orientation (111). Superlattice reflections (001), (110), (200), and (002) of ordered $L1_0$ FePt are also present, revealing that magnetically hard FePt phase formed fully if the deposition temperature exceeded 450 °C.[16] The crystal structure of sample C was similar to that indicated by combining the peaks for samples A and B. However, a Cr underlayer considerably reduced the intensity of FePt(111). The predominant orientation may be FePt(200) or FePt(002). The preferred orientation of the Cr underlayer is also (002). Comparing Fig. 1(c) with Fig. 1(a) demonstrates that the Cr(110) peak appears only after the FePt magnetic layer is deposited on the Cr underlayer. This finding is rather surprising. The ordered FePt(001) texture should intuitively grow epitaxially with the crystallographic Cr(002) ×[110]//FePt(001)[100],[17] because the lattice misfit[10] of Cr(002)/FePt(001) planes is only 5.8% that is smaller than that of the FePt(001)/MgO(100) planes. Therefore, the $L1_0$ FePt(001)[100] should grow epitaxially with Cr(002)[110]. However, randomly oriented $L1_0$ FePt phase structure was observed. Sample D exhibits only a single FePt(111) orientation. Pt is faced-centered cubic (fcc) with a (111) preferred orientation. The lattice constant is 3.92 Å, and is close to that of the faced-centered tetragonal (fct) ordered $L1_0$ FePt phase. The mismatch between FePt and Pt is only about 1.6%. Accordingly, FePt will grow well with Pt(111) to yield a single FePt(111) orientation. Sample D yielded no Pt(111) peak. The Pt layer is only 2 nm thick and the peak from this layer cannot easily be detected by XRD. Sample E contains a Cr underlayer and $L1_0$ FePt with a single orientation. Its diffraction pattern also reveals that the (001) texture is preserved throughout the $L1_0$ FePt layer by epitaxial growth between the Pt buffer layer and the FePt layer. Comparing the diffraction pattern of sample E with those of samples C and D indicates that the development of the $L1_0$ FePt(001) preferred orientation is governed by the presence of both the Cr underlayer and the Pt buffer layer. The results suggest that a mechanism at the interface of FePt/Cr and FePt/Pt/Cr is responsible for the preferred orientation of $L1_0$ FePt (001).

Figure 2 plots the room-temperature in-plane and the out-of-plane magnetization loops of samples B–E. These loops of samples B and D are similar because both samples exhibit the same preferred orientation (111). In sample C, the in-plane squareness ($S_{\|}$) slightly exceeds the out-of-plane squareness ($S_{\perp}$). Only sample E exhibits perpendicular magnetic anisotropy and an out-of-plane squareness ($S_{\perp}$) of about one. $S_{\perp}$ greatly exceeds $S_{\|}$. Its in-plane loop is not saturated at 1.2 T. Accordingly, the easy axis will be perpendicular to the film plane. Additionally, M_s of the $L1_0$ FePt phase in sample C was considerably reduced. M_s of samples B, D, and E is 200 emu/cm^3 higher than that of sample C (FePt/Cr), because Cr atoms diffuse from the underlayer into the FePt magnetic layer and they react strongly with the Fe and Pt atoms to produce some compounds at the FePt/Cr interface. M_s of FePt/Cr thin film with a 2 nm Pt buffer layer reached 700 emu/cm^3, and the FePt/Pt/Cr trilayer exhibited perpendicular magnetic anisotropy. Pt buffer layers are good barriers to the diffusion of the Cr atoms into the FePt layer.[14]

Figure 3 presents cross-sectional TEM images of samples C and E. In sample C, some variously sized amorphouslike regions [squares in Fig. 3(a)] were found at the FePt/Cr interface. TEM-EDX at point A in Fig. 3(a) reveals that most of the newly observed layer is Cr-rich FePtCr alloy. The structure of this alloy layer seems to be unrelated to the Cr underlayer and the FePt magnetic layer. Therefore, the FePtCr alloy impedes the epitaxial growth of $L1_0$ FePt(001) in the Cr(002) direction. The FePtCr alloy formed an epitaxial barrier. Unlike in Fig. 3(a), good epitaxial growth at the interfaces in the FePt/Pt/Cr trilayer was identified [Fig. 3(b)]. The orientations of the Cr underlayer, the Pt buffer layer, and the FePt magnetic layer were determined to be

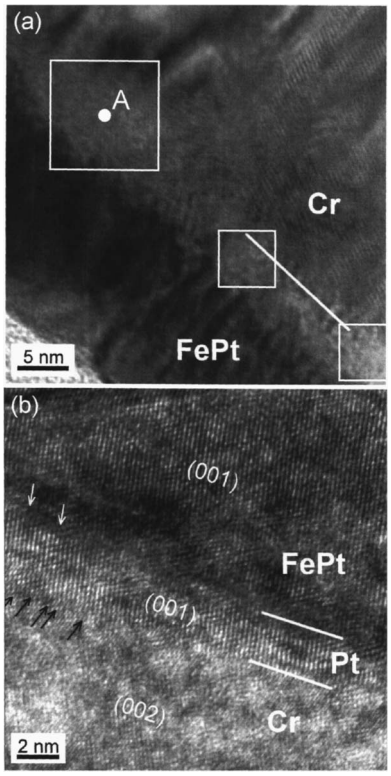

FIG. 3. Cross-section TEM images of (a) sample C (FePt/Cr bilayer) and (b) sample E (FePt/Pt/Cr trilayer).

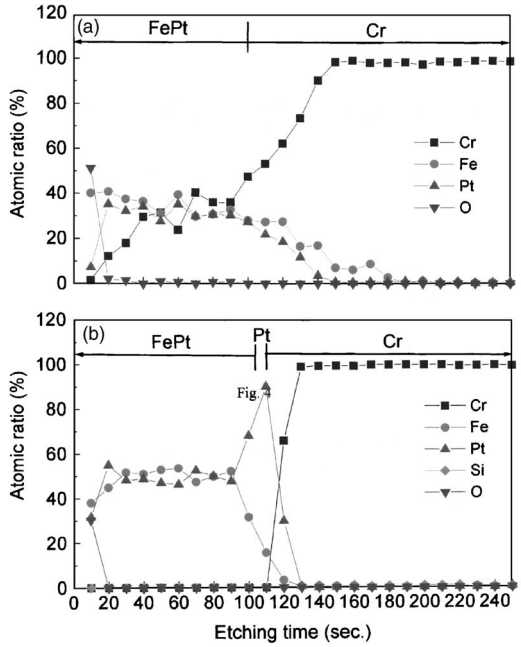

FIG. 4. AES depth profiles of (a) sample C (FePt/Cr bilayer) and (b) sample E (FePt/Pt/Cr trilayer).

(002), (001), and (001), respectively, indicating a good epitaxial growth from the Cr underlayer to the FePt magnetic layer. No FePtCr alloy epitaxial barrier forms at the interface when the Pt buffer layer is inserted. The lattice constant of Pt is 3.92 Å, between 4.08 Å for Cr and 3.86 Å for FePt, so the intermediate Pt layer significantly reduce the strains at the interface. Semicoherent interfaces and dislocations (black and white arrows) were found in the FePt/Pt and Pt/Cr interfaces that modulate the mismatch strain energy.[8,18] Therefore, the epitaxial growth can continue over a long distance.

The AES depth profiles of samples C and E were examined to clarify the effect of diffusion at the interface. Figure 4 displays the results. The Cr atoms diffused into the FePt layer in sample C, but not in sample E, revealing that the Pt buffer layer acts an effective barrier to the diffusion of Cr atoms into the FePt magnetic layer. Additionally, the diffusion depth of Fe atoms exceeds that of the Pt atoms. The Hume-Rothery rules[19] demonstrate that the atomic size, the crystal structure, and the electronegativity of Cr are similar to those of Fe, but not to those of Pt, suggesting that the CrFe alloy solidifies more easily than the CrPt alloy. Therefore, the main alloy of the epitaxial barrier is FeCr, not CrPt.

In summary, $L1_0$ FePt thin films with highly perpendicular magnetic anisotropy can be successfully fabricated with the inclusion of a Cr underlayer and a Pt buffer layer. The epitaxial growth of the FePt/Pt/Cr trilayer structure is perfect. However, the FePt/Cr(002) bilayer structure cannot produce the ordered $L1_0$ FePt with the (001) preferred orientation because the Cr atoms diffuse into the FePt magnetic layer. A CrFePt epitaxial barrier forms at the interface. An inserted Pt buffer layer impedes the diffusion of Cr atoms.

This work was supported by the Ministry of Economic Affairs, ROC under Contract No. 93-EC-17-A-08-S1-0006.

[1] Y. F. Ding, J. S. Chen, E. Liu, and J. P. Wang, J. Magn. Magn. Mater. **285**, 443 (2005).
[2] T. Suzuki, Z. Zhang, A. K. Singh, J. Yin, A. Perumal, and H. Osawa, IEEE Trans. Magn. **42**, 555 (2005).
[3] K. Kang, T. Suzuki, Z. G. Zhang, and C. Papusoi, J. Appl. Phys. **95**, 7273 (2004).
[4] M. L. Yan, R. Skomski, A. Kashyap, L. Gao, S. H. Liou, and D. J. Sellmyer, IEEE Trans. Magn. **40**, 2495 (2004).
[5] Y. K. Takahashi and K. Hono, Appl. Phys. Lett. **84**, 383 (2004).
[6] D. Weller *et al.*, IEEE Trans. Magn. **36**, 10 (2000).
[7] T. Shima, K. Takanashi, Y. K. Takahashi, and K. Hono, Appl. Phys. Lett. **85**, 2571 (2004).
[8] M. H. Hong, K. Hono, and M. Watanabe, J. Appl. Phys. **84**, 4403 (1998).
[9] M. Yu, Y. Lin, and D. J. Sellmyer, J. Appl. Phys. **87**, 6959 (2000).
[10] D. A. Porter and K. E. Easterling, *Phase Transformations in Metals and Alloys*, 2nd ed. (Stanley Thornes, Cheltenham, 2000), p. 156.
[11] K. Kang, Z. G. Zhang, T. Suzuki, and C. Papusoi, J. Appl. Phys. **95**, 7273 (2004).
[12] S. Jeong, M. E. McHenry, and D. E. Laughlin, IEEE Trans. Magn. **37**, 1039 (2001).
[13] Y. Xu, J. S. Chen, D. Dai, and J. P. Wang, IEEE Trans. Magn. **38**, 2042 (2002).
[14] J. S. Chen, Y. Xu, and J. P. Wang, J. Appl. Phys. **93**, 1661 (2003).
[15] Y. Xu, J. S. Chen, and J. P. Wang, Appl. Phys. Lett. **80**, 3325 (2002).
[16] A. C. Sun, P. C. Kuo, S. C. Chen, C. Y. Chou, H. L. Huang, and J. H. Hsu, J. Appl. Phys. **95**, 7624 (2004).
[17] T. Suzuki, N. Honda, and K. Ouchi, IEEE Trans. Magn. **35**, 2748 (1999).
[18] D. A. Porter and K. E. Easterling, *Phase Transformations in Metals and Alloys*, 2nd ed. (Stanley Thornes, Cheltenham, 2000), p. 145.
[19] J. F. Shackelford, *Introduction to Materials Science for Engineers*, 5th ed. (Prentice-Hall, New Jersey, 2000), p. 117.